Anomalous conductance spectrum in ferromagnet/d-wave superconductor junctions carrying a supercurrent

2008 J. Phys.: Condens. Matter 20 335212

(http://iopscience.iop.org/0953-8984/20/33/335212)

J. Phys.: Condens. Matter **20** (2008) 335212 (6pp) doi:10.1088/0953-8984/20/33/335212

Anomalous conductance spectrum in ferromagnet/d-wave superconductor junctions carrying a supercurrent

Li-Yun Yang[1,3] **and Jie Liu**[1,2]

[1] Institute of Applied Physics and Computational Mathematics, PO Box 8009 (28), Beijing 100088, People's Republic of China
[2] Center for Applied Physics and Technology, Peking University, Beijing 100084, People's Republic of China
[3] Department of Physics, Beijing Normal University, Beijing 100875, People's Republic of China

Received 2 February 2008
Published 22 July 2008
Online at stacks.iop.org/JPhysCM/20/335212

Abstract

The Blonder–Tinkham–Klapwijk approach is exploited to study the conductance spectrum in ferromagnet(F)/d-wave superconductor(S) junctions with a transverse supercurrent in S. In the absence of exchange energy with (110) contact ($\alpha = \pi/4$), when the supercurrent $q \neq 0.0$, we find that the conductance coherence peaks split into subpeaks at $Z = 0.5$ and 1.0. The energy difference between the two subpeaks corresponding to a single coherence peak is found to increase as the supercurrent increases. For the F/S junctions with (110) contact at $Z = 0.5$ and 1.0, when the supercurrent $q \neq 0.0$ the subpeaks split again: in this the exchange energy plays a dominant role, similar to the Zeeman effect. At certain values of h_0/E_F, we found that the two Zeeman-like peaks around zero energy could merge into a single one.

1. Introduction

Conductance characteristics in normal metal (or ferromagnet)/superconductor (N (or F)/S) tunnel junctions have recently attracted much attention in experimental and theoretical investigations [1–18]. This is partly because tunneling spectroscopy can provide a lot of information towards completely understanding the superconducting mechanism. The Andreev reflection (AR) process [19] plays an important role in tunneling spectroscopy. In this process, an electron in the normal metal impinging on the N/S interface is Andreev reflected and converted into a hole moving in the opposite direction, and a Cooper pair is carried away in the superconductor. Andreev reflection near the Fermi level conserves energy and momentum but does not conserve total spin, that is, the incoming electron and the Andreev reflected hole occupy opposite spin bands. In ferromagnet/superconductor (F/S) junctions, AR still occurs and however is strongly suppressed by the spin polarization of the electrons in ferromagnet [20, 21]. It is recognized that in such F/S junctions, conducting electrons with up and down spins experience different potentials in the ferromagnet and therefore the properties of the junction have a strong dependence on the exchange energy in the ferromagnet. An electron in the F is Andreev reflected from the F/S interface as a hole along an approximately time-reversed path, where the time-reverse symmetry has been broken by the presence of the F.

It is interesting to study tunneling spectroscopy when a transverse supercurrent I_S passes through a superconductor. It was found experimentally that the pair correlations are weakened by the supercurrent, leading to a modification of the density of states (DOS) corresponding to the tunneling spectra and leading to a reduction of the gap [22]. With increasing I_S the coherence peaks were suppressed and broadened: here the role of the supercurrent is similar to an external magnetic field. The conductance characteristics of a clean N/S junction with an I_S in S parallel to the interface have been studied theoretically [23]. Near critical I_S, and for $Z \simeq 1$, a three-humped structure appears, signaling the onset of current-induced removal of the gap on the Fermi surface where gap originally exists [23]. Similar characteristics of the conductance described in the above should exist in the F/d-wave S junctions. In addition, due to the existence of the exchange energy of F and the anisotropy of d-wave S, we expect some distinct phenomena to emerge.

Because the cuprate superconductors with high critical temperature have a $d_{x^2-y^2}$-wave symmetry of pair poten-

tial [24], the study of F/d-wave S junctions has become an important topic. The pair potential for $d_{x^2-y^2}$-wave symmetry has a $\cos 2\theta$ dependence, resulting in a number of interesting phenomena. For example, for the {110}-orientation, the amplitude of the pair potential disappears for $\theta = \pi/4$. In this case, the d-wave symmetry could lead to a sizable areal density of midgap states [25], which is the origin of the zero-bias conductance peak observed in most high-T_c superconductor junctions. This feature can be used to distinguish between d-wave and anisotropic s-wave superconductors [25]. As stated above, tunneling spectroscopy depends on the orientation of the S crystal with respect to the interface normal. When the c axis is parallel to the interface normal, the F/d-wave S junction is a three-dimension (3D) system, in contrast when the c axis is along a direction within the interface, it may effectively be regarded as a 2D system. In the latter case, the angle between the a axis and the interface normal α also plays an important role in tunneling spectroscopy. Such an orientation dependence of tunneling spectroscopy is another motivation of this work.

When a uniform supercurrent I_S passes through a conventional three-dimensional S, the phase of $\Delta(\mathbf{k})$ has a spatial variation as $e^{2i\mathbf{q_s}\cdot\mathbf{r}}$, where $\mathbf{r}$ is the center-of-mass position of a Cooper pair, $\mathbf{q_s} = (m^*\mathbf{v_s}/2\hbar)$, with $\mathbf{v_s}$ the supercurrent velocity, and m^* the mass of the Cooper pair. This spatially varying phase leads to an anisotropic quasiparticle excitation spectrum in a clean S [23]. In a two-dimensional d-wave S, the Δ_q versus q relation also depends on the directions of the supercurrent (Δ_q denotes the maximum gap in the presence of I_S). Superconductivity disappears as I_S reach the critical current. At zero temperature ($T = 0$), when q is less than $0.3\Delta^0$ ($q \equiv q_s/k_F$, $\Delta^0 \equiv \Delta_0/E_F$, here Δ_0 is the maximum superconducting gap when $T = 0$, $I_S = 0$; k_F and E_F are the Fermi momentum and energy, respectively), the changes of the order parameter Δ_q of a two-dimensional d-wave S with q in both the antinodal ($\alpha = 0$) and nodal ($\alpha = \pi/4$) directions are almost the same. However, a great difference exists for large q. When I_S is along the antinodal directions, Δ_q has a sharp drop between $q = 0.384\Delta^0$ and $0.385\Delta^0$. After that it drops continuously to zero at $q = 0.53\Delta^0$. When $\alpha = \pi/4$, Δ_q gradually decreases to $0.689\Delta^0$ at $q = 0.469\Delta^0$, and has no solution beyond. The thermodynamic critical supercurrent density $j_s = 0.238 env_F\Delta^0$ ($0.225\ env_F\Delta^0$) is reached at $q = q_c \approx 0.35\Delta^0$ ($0.39\Delta^0$) for a current in the antinodal (nodal) direction [23].

Our paper is organized as follows. In section 2 we adopt the BdG equation to study F/d-wave S junctions carrying a transverse supercurrent I_S for (100) and (110) contact. The BTK theory is readily extended to the spin-dependent transport through an F/d-wave S junction, and the differential conductance is derived. Our main results on conductance spectrum structure are presented in section 3. It is found that the conductance spectrum shows many interesting properties that are distinct from that in N(or F)/s-wave S junctions. Section 4, is our conclusion.

2. Model and theory

We consider an F/S junction structure of semi-infinite F and d-wave S carrying a supercurrent separated by a very thin insulating layer located at $x = 0$, as shown in figure 1. If the c-axis of the d-wave S is along a direction within plane $x = 0$, which is taken to be the z-axis, such an F/d-wave S junction may be regarded as a two-dimensional system. The ferromagnet is described by an effective single-particle Hamiltonian for spin-polarized electrons with exchange energy h_0, the superconductor is assumed to be d-wave pairing and described by a BCS-like Hamiltonian, and the insulating layer described by a δ-type potential $V(x) = U\delta(x)$, where U depends on the product of barrier height and width. For simplicity, the effective masses m in both F and S are assumed to be identical. The d-wave pair potential is a function of the angle θ_S between the quasiparticle wavevector and the interface normal, given by $\Delta(x) = \Delta^d_{\pm} = \Delta_0\cos(2\theta_S \mp 2\alpha)$ for $x > 0$ when $T = 0$, where Δ^d_+ (Δ^d_-) stands for the pair potential for electron-like (hole-like) quasiparticles [27], Δ_0 is a constant, and α is the angle between the a-axis of the crystal and the interface normal. $\alpha = \pi/4$ for the interface normal along the [110] orientation and $\alpha = 0$ for the interface normal along [100] orientation. $\Delta(x) = 0$ in the F region for $x < 0$. Notice that the effective pair potentials experienced by the electron-like and hole-like quasiparticles in the d-wave S are usually different, and can even have opposite signs under certain circumstances.

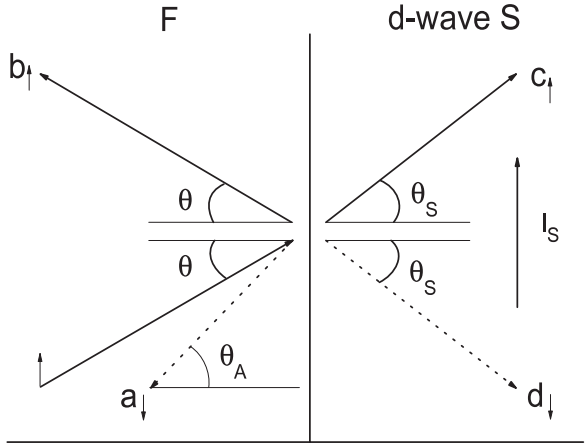

Figure 1. The Schematic sketch of our model, with a uniform supercurrent I_S in a d-wave superconductor side parallel to the ferromagnet/superconductor interface. The solid-line arrow stands for the electron with spin-σ in F or electron-like quasiparticle in S, while the dotted-line arrow for the hole with spin-$\bar{\sigma}$ in F or hole-like quasiparticle in S.

We adopt the BdG equation [28] to study the F/d-wave S junction. This approach has been widely used to describe quasiparticle states in superconductors with spatially varying pair potentials. In the F/S junction, the quasiparticle states are generally expressed by wavefunctions of four components, respectively, for electron-like quasiparticle (ELQ) and hole-like quasiparticle (HLQ) with spin up and down. In the absence of spin-flip scattering, the four-component BdG equations may be decoupled into two sets of two-component equations: one for the spin-up electron-like and spin-down hole-like quasiparticle wavefunctions $(u_\uparrow, v_\downarrow)$, the other for $(u_\downarrow, v_\uparrow)$.

The BdG equation is given by

$$\begin{bmatrix} H_0(\mathbf{r}) - \eta_\sigma h(\mathbf{r}) & \Delta(\mathbf{r}) \\ \Delta^*(\mathbf{r}) & -H_0(\mathbf{r}) - \eta_\sigma h(\mathbf{r}) \end{bmatrix} \begin{bmatrix} u_\sigma(\mathbf{r}) \\ v_{\bar\sigma}(\mathbf{r}) \end{bmatrix} = E \begin{bmatrix} u_\sigma(\mathbf{r}) \\ v_{\bar\sigma}(\mathbf{r}) \end{bmatrix}. \quad (1)$$

Here $H_0(\mathbf{r}) = -\hbar^2\nabla_r^2/2m + V(\mathbf{r}) - E_\mathrm{F}$ with $V(\mathbf{r})$ the usual static potential, E is the quasiparticle energy relative to the Fermi energy E_F. $h(\mathbf{r}) = h_0\Theta(-x)$ with h_0 the exchange energy in F and $\Theta(x)$ is the unit step function, $\eta_\sigma = 1$ for $\sigma = \uparrow$ and -1 for $\sigma = \downarrow$, and $\bar\sigma$ stands for the spin opposite to σ. $\Delta(\mathbf{r}) = \Delta(T)\Theta(x)$ is the temperature-dependent energy gap that follows the BCS relation $\Delta(T) = \Delta_0\cos(2\theta_\mathrm{S} \mp 2\alpha)\tanh[1.76(T_\mathrm{c}/T - 1)]$ where T_c is the critical temperature of the d-wave S.

In the WKBJ approximation, equation (1) has special solutions of the form

$$\begin{pmatrix} u_\sigma(\mathbf{r}) \\ v_{\bar\sigma}(\mathbf{r}) \end{pmatrix} = \mathrm{e}^{\mathrm{i}\mathbf{k}\cdot\mathbf{r}} \begin{pmatrix} u^0_\sigma(\mathbf{r})\mathrm{e}^{\mathrm{i}\mathbf{q_s}\cdot\mathbf{r}} \\ v^0_{\bar\sigma}(\mathbf{r})\mathrm{e}^{-\mathrm{i}\mathbf{q_s}\cdot\mathbf{r}} \end{pmatrix}, \quad (2)$$

where $u^0_\sigma(\mathbf{r})$ and $v^0_{\bar\sigma}(\mathbf{r})$ obey the generalized Andreev equations [19],

$$\left[\frac{\hbar^2}{2m}(\mathbf{k}+\mathbf{q_s})^2 - \eta_\sigma h_0\Theta(-x)\right]u^0_\sigma(\mathbf{r}) - \frac{\mathrm{i}\hbar^2(\mathbf{k}+\mathbf{q_s})}{m}\cdot\nabla u^0_\sigma(\mathbf{r}) + \Delta(\mathbf{r})\Theta(x)v^0_{\bar\sigma}(\mathbf{r}) = Eu^0_\sigma(\mathbf{r}), \quad (3)$$

$$-\left[\frac{\hbar^2}{2m}(\mathbf{k}-\mathbf{q_s})^2 + \eta_\sigma h_0\Theta(-x)\right]v^0_{\bar\sigma}(\mathbf{r}) + \Delta^*(\mathbf{r})\Theta(x)u^0_\sigma(\mathbf{r}) + \frac{\mathrm{i}\hbar^2(\mathbf{k}-\mathbf{q_s})}{m}\cdot\nabla v^0_{\bar\sigma}(\mathbf{r}) = Ev^0_{\bar\sigma}(\mathbf{r}). \quad (4)$$

Obviously, the eigenenergy E is symmetric about $\hbar^2\mathbf{q_s}\cdot\mathbf{k}/m$ rather than zero. This leads to different energy gaps for different electron directions. For simplicity, uniform I_S in S is assumed to be parallel to the interface in this work.

Suppose a beam of spin-σ ELQ incident on the interface at $x = 0$ at an angle θ from F to S. There are four possible trajectories (as shown in figure 1): normal reflection (NR) b_1^σ at angle θ, Andreev reflection (AR) [19] $a_1^{\bar\sigma}$ as a hole with spin-$\bar\sigma$ at angle θ_A, and transmission c_1^σ and $d_1^{\bar\sigma}$ to S at angle θ_S, respectively, as a spin-σ ELQ and a spin-$\bar\sigma$ HLQ. It is worth pointing out that the AR coefficient $a_1^{\bar\sigma}$ is labeled with $\bar\sigma$ because the AR results in an electron deficiency in the spin-$\bar\sigma$ subband of the F, even though it is at times called a spin-σ hole. With general solutions of the BdG equation, the wavefunctions in F and S regions can be obtained. Owing to translational invariance in directions parallel to the interface, the wavefunctions in the F and S are given by

$$\Psi^\mathrm{F}_{1\sigma} = \begin{pmatrix} 1 \\ 0 \end{pmatrix}\mathrm{e}^{\mathrm{i}q_\mathrm{e}^\sigma x\cos\theta} + a_1^{\bar\sigma}\begin{pmatrix} 0 \\ 1 \end{pmatrix}\mathrm{e}^{\mathrm{i}q_\mathrm{h}^{\bar\sigma} x\cos\theta_\mathrm{A}} + b_1^\sigma\begin{pmatrix} 1 \\ 0 \end{pmatrix}\mathrm{e}^{-\mathrm{i}q_\mathrm{e}^\sigma x\cos\theta}, \quad (5)$$

for $x \leqslant 0$, and

$$\Psi^\mathrm{S}_{1\sigma} = c_1^\sigma\begin{pmatrix} u_+^d\mathrm{e}^{\mathrm{i}\phi_+^d} \\ v_+^d \end{pmatrix}\mathrm{e}^{\mathrm{i}k_\mathrm{e}^d x\cos\theta_\mathrm{S}} + d_1^{\bar\sigma}\begin{pmatrix} v_-^d\mathrm{e}^{\mathrm{i}\phi_-^d} \\ u_-^d \end{pmatrix}\mathrm{e}^{-\mathrm{i}k_\mathrm{h}^d x\cos\theta_\mathrm{S}}, \quad (6)$$

for $x \geqslant 0$. In equations (5),

$$q_\mathrm{e}^\sigma = k_\mathrm{F}\sqrt{1 + \left[h_0 - \hbar^2 q_s^2/2m + E'\right]/E_\mathrm{F}}, \quad (7a)$$

$$q_\mathrm{h}^{\bar\sigma} = k_\mathrm{F}\sqrt{1 + \left[-h_0 - \hbar^2 q_s^2/2m - E'\right]/E_\mathrm{F}}, \quad (7b)$$

indicating different Fermi wavevectors for the spin-σ electrons and spin-$\bar\sigma$ holes in F, with $E' = E - \hbar^2 k_\mathrm{F} q_s\sin\theta/m$. In equation (6),

$$k_\mathrm{e}^d = k_\mathrm{F}\sqrt{1 + \left[-\hbar^2 q_s^2/2m + \Omega_+\right]/E_\mathrm{F}}, \quad (8a)$$

$$k_\mathrm{h}^d = k_\mathrm{F}\sqrt{1 - \left[-\hbar^2 q_s^2/2m + \Omega_-\right]/E_\mathrm{F}}. \quad (8b)$$

Here $k_\mathrm{F} = \sqrt{2mE_\mathrm{F}/\hbar^2}$ is the Fermi wavevector in S, $u_\pm^d = \sqrt{(1+\Omega_\pm/E')/2}$, $v_\pm^d = \sqrt{(1-\Omega_\pm/E')/2}$ with $\Omega_\pm = \sqrt{E'^2 - \Delta_\pm^2}$, and $\phi_\pm^d = \cos^{-1}[\cos(2\theta_\mathrm{S}\mp2\alpha)/|\cos(2\theta_\mathrm{S}\mp2\alpha)|]$. In the BTK approach [29], since the wavevector component parallel to the interface is assumed to remain unchanged in the reflection and transmission processes, the angles θ, θ_A and θ_S differ from each other except when $\theta = 0$. All the coefficients $a_1^{\bar\sigma}$, b_1^σ, c_1^σ and $d_1^{\bar\sigma}$ can be determined by matching the boundary conditions at $x = 0$: $\Psi^\mathrm{F}_{1\sigma}(0) = \Psi^\mathrm{S}_{1\sigma}(0)$ and $(\mathrm{d}\Psi^\mathrm{S}_{1\sigma}/\mathrm{d}x)_{x=0} - (\mathrm{d}\Psi^\mathrm{F}_{1\sigma}/\mathrm{d}x)_{x=0} = 2k_\mathrm{F}Z\Psi^\mathrm{F}_{1\sigma}(0)$, where $Z = mU/k_\mathrm{F}$ is a dimensionless parameter describing the magnitude of interfacial resistance. The Andreev and normal reflection coefficients $a_1^{\bar\sigma}$ and b_1^σ are given below,

$$a_1^{\bar\sigma} = \frac{1}{A}2q_\mathrm{e}^\sigma\cos\theta(k_\mathrm{e}\cos\theta_\mathrm{S} + k_\mathrm{h}\cos\theta_\mathrm{S}), \quad (9)$$

$$b_1^\sigma = \frac{1}{A}[(q_\mathrm{e}^\sigma\cos\theta - k_\mathrm{e}\cos\theta_\mathrm{S} - 2\mathrm{i}k_\mathrm{F}\cos\theta Z) \times (k_\mathrm{h}\cos\theta_\mathrm{S} + q_\mathrm{h}^{\bar\sigma}\cos\theta_\mathrm{A} - 2\mathrm{i}k_\mathrm{F}\cos\theta Z)B_+ + \left(k_\mathrm{e}\cos\theta_\mathrm{S} - q_\mathrm{h}^{\bar\sigma}\cos\theta_\mathrm{A} + 2\mathrm{i}k_\mathrm{F}\cos\theta Z\right) \times \left(k_\mathrm{h}\cos\theta_\mathrm{S} + q_\mathrm{e}^\sigma\cos\theta - 2\mathrm{i}k_\mathrm{F}\cos\theta Z\right)B_-], \quad (10)$$

here,

$$A = (q_\mathrm{e}^\sigma\cos\theta + k_\mathrm{e}\cos\theta_\mathrm{S} + 2\mathrm{i}k_\mathrm{F}\cos\theta Z) \times \left(q_\mathrm{h}^{\bar\sigma}\cos\theta_\mathrm{A} + k_\mathrm{h}\cos\theta_\mathrm{S} - 2\mathrm{i}k_\mathrm{F}\cos\theta Z\right)B_+ + \left(q_\mathrm{h}^{\bar\sigma}\cos\theta_\mathrm{A} - k_\mathrm{e}\cos\theta_\mathrm{S} - 2\mathrm{i}k_\mathrm{F}\cos\theta Z\right) \times \left(k_-^d\cos\theta_\mathrm{S} - q_\mathrm{e}^\sigma\cos\theta - 2\mathrm{i}k_\mathrm{F}\cos\theta Z\right)B_-, \quad (11)$$

$$B_\pm = \frac{\Delta_\pm\mathrm{e}^{\mathrm{i}\phi_\pm^d}}{E' \mp \Omega_\pm}. \quad (12)$$

The tunneling conductance of an normal metal (N)/s-wave S junction has been given by the BTK theory [29], with the contribution of AR being included. In this work the BTK approaches readily extended to the spin-dependent

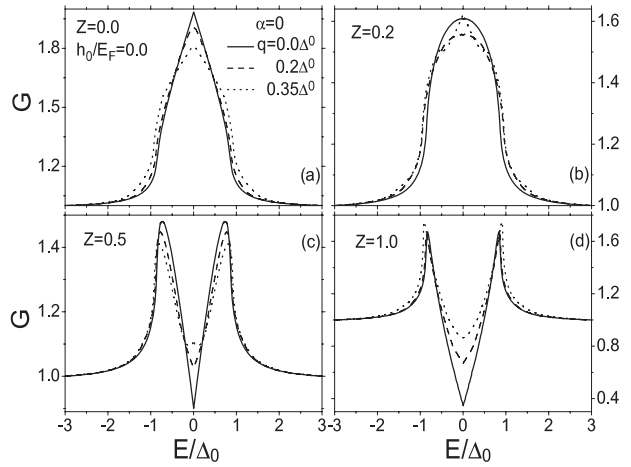

Figure 2. Normalized conductance spectra for normal metal/d-wave superconductor junctions for different $Z = 0$ (a), $Z = 0.2$ (b), $Z = 0.5$ (c) and $Z = 1.0$ (d), with $q \equiv q_s/k_F = 0.0\Delta^0$ (solid line), $q = 0.2\Delta^0$ (dashed line) and $q = 0.35\Delta^0$ (dotted line). Here the angle between the a axis and the interface normal $\alpha = 0$ (i.e. (100) contact).

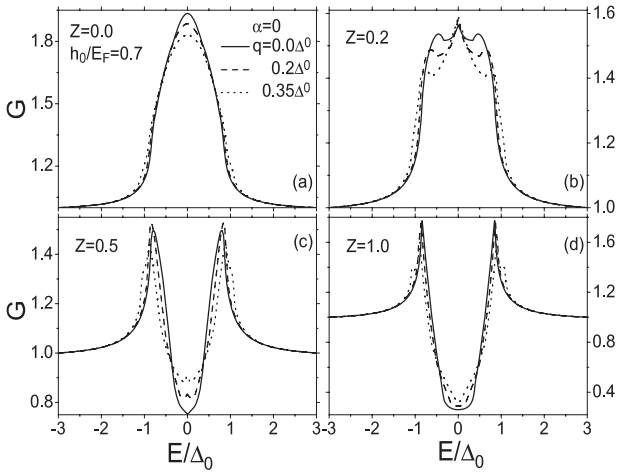

Figure 3. Normalized conductance spectra for ferromagnet/d-wave superconductor junctions with (100) contact for different Z and q with $h_0/E_F = 0.7$. The other parameters are the same as in figure 2.

transport through an F/d-wave S junction, and the differential conductance is given by [1, 24]

$$G(\theta) = G_\uparrow + G_\downarrow = \frac{e^2}{\pi\hbar}\,\mathrm{Re}\sum_{\sigma=\uparrow,\downarrow} P_\sigma\left(1 + \frac{q_h^{\bar\sigma}\cos\theta_A}{q_e^{\sigma}\cos\theta}\left|a_1^{\bar\sigma}\right|^2 - \left|b_1^{\sigma}\right|^2\right), \qquad (13)$$

where $P_\sigma = (E_F + \eta_\sigma h_0)/2E_F$ is the polarization for spin-σ in the F. In the experiments, the measured conductance is given by a weighted average over contributions from all possible electron trajectories,

$$G = \frac{1}{2}\int_{-\infty}^{\infty} \mathrm{d}E \int_{-\frac{\pi}{2}}^{\frac{\pi}{2}} \mathrm{d}\theta\, G(\theta)\cos\theta \frac{\partial f(E - eV)}{\partial E}. \qquad (14)$$

Here, $f(E)$ is the Fermi distribution function.

3. Results and discussions

In what follows we discuss numerical results from equations (13) and (14) together with equations (9)–(12). Let us first study the effect of supercurrent in the S on the conductance spectrum in the absence of exchange energy by taking the finite temperature $T = 0.6T_C$. Figure 2 shows the normalized conductance G versus dimensionless energy E/Δ_0, for various $Z \equiv mU/k_F$, and $q \equiv q_s/k_F$ for N/d-wave S junctions with (100) contact (i.e. $\alpha = 0$, $\Delta_\pm^d = \Delta_0\cos(2\theta_S)$). Equations (13) shows that while ordinary reflection reduces the current, Andreev reflection increases it by giving up to two transferred electrons (a Cooper pair) for one incident electron. So within the superconducting gap at zero temperature the dimensionless differential conductance exhibits a central peak at $|E| = 0.0$. When a uniform supercurrent I_S passes through a two-dimensional d-wave S, the phase of $\Delta(\mathbf{k})$ has a spatial variation as $e^{2i\mathbf{q}_s\cdot\mathbf{r}}$. This spatially varying phase leads to an anisotropic quasiparticle excitation spectrum in a clean S besides the intrinsic anisotropic property. For $Z = 0.0$, as shown in figure 2(a), the central peak due to Andreev reflection is gradually suppressed and broadened by increasing q. With increasing barrier strength Z, Andreev reflection is greatly suppressed, so conductance within the energy gap diminishes rapidly and there are two sharp peaks in the conductance spectrum at $|E| \approx \Delta_0$, called coherence peaks. From figure 2(d), it is clear that barrier strengths $Z \sim 1.0$ give results essentially indistinguishable from those for classical tunnel junctions where G exhibits a central dip. When $q \neq 0$, the eigenenergy E is symmetric about $\hbar^2\mathbf{q}_s\cdot\mathbf{k}/m$ rather than zero. The energy corresponding to the coherence peaks is determined by $|E| - \hbar^2\mathbf{q}_s\cdot\mathbf{k}/m \approx \Delta_0$. As q increases, the coherence peaks are broadened, and the peaks move outward while the gap diminishes, again because of the gap anisotropy caused by the supercurrent. Interestingly, one sees an intricate behavior with some similarity to the corresponding cases in metal/s-wave S junctions [30], where a three peaks structure including a peak at zero energy at nearly critical I_S and $Z \approx 0.5$ appears in the conductance, indicating the onset of current-induced removal of the gap on the Fermi surface where a gap originally exists [23]. The central peak disappears at $Z \gg 0.5$ because the Andreev reflection which induces this peak is hypersensitive to Z. The remaining effect of current-induced gap anisotropy and the eventual disappearance of the gap are largely obscured by the d-wave anisotropy.

For F/d-wave S junctions with (100) contact, by taking the same parameters as figure 2, the calculated results for exchange energy $h_0/E_F = 0.7$ are shown in figure 3. In addition to the same results as figure 2, where the transverse supercurrent will also slightly lowers the coherence peaks and a three peaks structure appears, some other interesting results are found. Comparing figures 3(d) and 2(d), one can find that with increasing q, the superconducting gap diminishes and this effect is suppressed by exchange energy.

The normalized conductance for (110) contact ($\alpha = \pi/4$, $\Delta_\pm^d = \cos(2\theta_S \mp 2\alpha) = \pm\sin(2\theta_S)$) is shown in figures 4 and 5, corresponding to the normal metal and ferromagnet

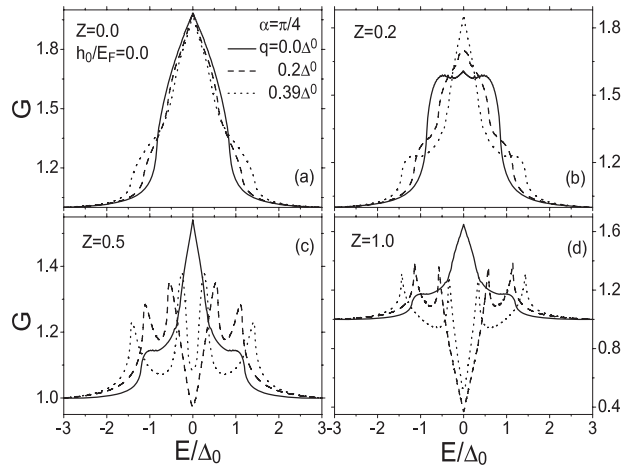

Figure 4. Normalized conductance spectra for normal metal/d-wave superconductor junctions for different $Z = 0.0$ (a), $Z = 0.2$ (b), $Z = 0.5$ (c) and $Z = 1.0$ (d), with $q \equiv q_s/k_F = 0.0\Delta^0$ (solid line), $q = 0.2\Delta^0$ (dashed line) and $q = 0.39\Delta^0$ (dotted line). Here the angle between the a axis and the interface normal $\alpha = \pi/4$ (i.e. (110) contact).

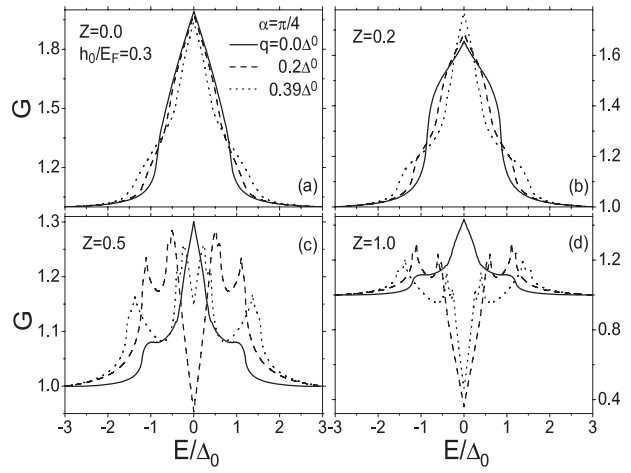

Figure 5. Normalized conductance spectra for ferromagnet/d-wave superconductor junctions with (110) contact for different Z and q with $h_0/E_F = 0.3$. The other parameters are the same as in figure 4.

junctions, respectively. In the absence of exchange energy [23], as shown in figure 4, besides the similar behavior to the corresponding cases in figure 2, three interesting features are found. First, for $Z = 0.5$ and 1.0 (as shown in figures 4(c) and (d)), the coherence peak is split into two subpeaks due to the presence of the transverse supercurrent in S, and the peak splitting increases as the supercurrent q increases. This may be understood by the following argument. For the case of a finite transverse supercurrent, there is an energy splitting E' in the energy between the spin-up and spin-down Bogoliubov fermions and that consequently leads to the splitting of the conductance peaks. The energy difference between the two subpeaks in the conductance spectrum is derived from the integral over θ of $2E'$, so with increasing q, the distance of the two subpeaks increase. Second, unlike metal/d-wave superconductor junctions with (100) contact for $Z = 0.5$ and

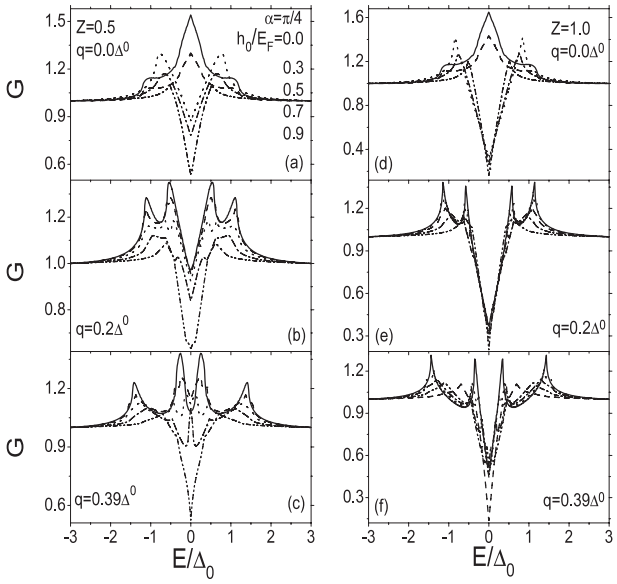

Figure 6. Normalized conductance spectra for ferromagnet/d-wave superconductor junctions for different $Z = 0.5$ (a), (b), (c), $Z = 1.0$ (d), (e), (f), with $q = 0.0\Delta^0$ (a), (d), $q = 0.2\Delta^0$ (b), (e) and $q = 0.39\Delta^0$ (c), (f), for various $h_0/E_F = 0.0$ (solid line), 0.3 (dashed line), 0.5 (dotted line), 0.7 (dash–dotted line) and 0.9 (dash–dot–dotted line).

critical q, zero-energy peak structures do not appear. Third, in the tunneling limit ($Z \geqslant 0.5$), with increasing q the zero-bias conductance peaks (ZBCPs) disappear and the conductance spectra show a zero-bias conductance dip (ZBCD) structure.

Figure 5 shows the normalized conductance for (110) contact in the presence of exchange energy, here $h_0/E_F = 0.3$, by taking the other parameters the same as in figure 4. For $Z = 0.5$, $Z = 1.0$ and $q \neq 0$, (as shown in figures 5(c) and (d)), the very interesting result is that the subpeak is split into two peaks, again due to the exchange energy together with the transverse supercurrent. Moreover, we find that a zero-energy peak structure appears at certain values of h_0/E_F, as explained below.

Figure 6 gives the calculation results of the normalized conductance for different exchange energy h_0/E_F by taking different Z and q with $\alpha = \pi/4$. It is shown that the coherence peak splits into two subpeaks when $q \neq 0.0$ with $Z = 0.5$ and 1.0 (as shown in figures 6(b), (c), (e) and (f)). The splitting energy is fixed for fixed q, and it is increased with increasing q. When the exchange energy $h_0/E_F \neq 0.0$ and the supercurrent $q \neq 0.0$, the subpeak splits into two peaks again (here it is called the Zeeman-like splitting). The Zeeman-like splitting energy is derived from the exchange energy together with the transverse supercurrent, and it is apparent that for fixed q that,the larger the exchange energy, the larger the energy difference between the two Zeeman-like splitting peaks in the conductance spectrum is. It is easy to understand that the exchange energy plays a dominant role in the Zeeman-like splitting, similar to in Zeeman splitting. Increasing the exchange energy from $h_0/E_F = 0.0$ to 0.9, the distance between the two peaks around $E = 0.0$ is decreased. At a certain value of h_0/E_F, these two peaks could merge into

a single one at zero energy (as shown in figure 6(c), when $h_0/E_F = 0.7$, a zero-energy peak appears in the conductance spectrum where a zero-energy dip originally appears), then the system become gapless.

4. Summary

In summary, we have studied the tunneling spectroscopy of a ferromagnet/d-wave superconductor carrying a transverse supercurrent I_S for (100) and (110) contact using the BdG equation. It is found that a uniform supercurrent I_S could lead to an anisotropic quasiparticle excitation spectrum in a clean S. For $\alpha = 0$, we observe a three-peak structure (one peak locates at zero energy) at nearly critical I_S and $Z \approx 0.5$ for both normal metal/superconductor (N/S) and ferromagnet/superconductor (F/S) junctions, signaling the onset of current-induced removal of the gap on the Fermi surface where a gap originally exists. For (110) contact, in the absence of exchange energy for the tunneling limit (i.e., $Z = 0.5$ and 1.0), one coherence peak splits into two subpeaks due to the presence of the transverse supercurrent in S, and the corresponding energy splitting increases as the supercurrent increases. For F/S junctions with (110) contact, when $q \neq 0.0$ with $Z = 0.5$ and 1.0, these subpeaks split again, namely, Zeeman-like splitting. The Zeeman-like splitting energy is dependent on both exchange energy and transverse supercurrent, while we find the exchange energy play a dominant role. Moreover, at certain values of h_0/E_F, we find that the two Zeeman-like peaks around zero energy could merge into single one.

Acknowledgments

This work is supported by National Natural Science Foundation of China under Grant No. 10725521, the National Fundamental Research Programme of China under Grant Nos. 2006CB921400, 2007CB814800.

References

[1] Tsuei C C and Kirtley J R 2000 *Rev. Mod. Phys.* **72** 969 and references therein
[2] Deutscher G 2005 *Rev. Mod. Phys.* **77** 109 and references therein
[3] Fischer Ø, Kugler M, Maggio-Aprile I and Berthod C 2007 *Rev. Mod. Phys.* **79** 353 and references therein
[4] Tedrow P W and Meservery R 1971 *Phys. Rev. Lett.* **26** 1921
[5] Meservey R and Tedrow P M 1994 *Phys. Rep.* **238** 173
[6] Prinz G A 1995 *Phys. Today* **48** 58
[7] de Jong M J M and Beenadder C W J 1995 *Phy. Rev. Lett.* **74** 1657
[8] Fogelström M, Rainer D and Sauls J A 1997 *Phy. Rev. Lett.* **79** 281
[9] Wei J Y T, Tsuei C C, van Bentum P J M, Xiong Q, Chu C W and Wu M K 1998 *Phys. Rev.* B **57** 3650
[10] Takahashi S, Imamura H and Maekawa S 1999 *Phys. Rev. Lett.* **82** 3911
[11] Žutić I and Valls O T 2000 *Phys. Rev.* B **61** 1555
[12] Xia K, Kelly P J, Bauer G E W and Turek I 2002 *Phys. Rev. Lett.* **89** 166603
[13] Kohen A, Leibovitch G and Deutscher G 2003 *Phys. Rev. Lett.* **90** 207005
[14] Zhang D and Ting C S 2003 *Phys. Rev.* B **67** 100506
[15] Wang Q, Chen H-Y, Hu C-R and Ting C S 2006 *Phys. Rev. Lett.* **96** 117006
[16] Bhattacharjee S and Sengupta K 2006 *Phys. Rev. Lett.* **97** 217001
[17] Yokoyama T and Tanaka Y 2007 *Phys. Rev.* B **75** 132503
[18] Lukic V and Nicol E J 2007 *Phys. Rev.* B **76** 144508
[19] Andreev A F 1964 *Phys. JETP* **19** 1228
[20] Soulen R J Jr *et al* 1998 *Science* **282** 85
[21] Upadgyay S K *et al* 1998 *Phys. Rev. Lett.* **81** 3247
[22] Anthore A, Pothier H and Esteve D 2003 *Phys. Rev. Lett.* **90** 127001
[23] Zhang D G, Ting C S and Hu C-R 2004 *Phys. Rev.* B **70** 172508
[24] Kashiwaya S and Tanaka Y 2000 *Rep. Prog. Phys.* **63** 1641
[25] Hu C R 1994 *Phys. Rev. Lett.* **72** 1526
[26] Bardeen J 1962 *Rev. Mod. Phys.* **34** 667
Maki K 1969 *Superconductivity* ed R D Parks (New York: Dekker)
[27] Yang L Y, Zheng Z M, Yu H L, Sun G Y and Xing D Y 2004 *Eur. Phys. J.* B **39** 377–84
[28] de Gennes P G 1966 *Superconductivity of Metals and Alloys* (New York: Benjamin)
[29] Blonder G E, Tinkham M and Klapwijk T M 1982 *Phys. Rev.* B **25** 4515
[30] Yang L-Y, Xing D Y, Li H-M and Liu J 2007 *Solid State Commun.* **143** 373–7